Assessment of Long-Term Water Absorption on Thermal, Mor-Phological and Mechanical Properties of Polypropylene-Based Composites With Agro-Waste Fillers

Tatiana Zhiltsova , Andreia Costa , Mónica S. A. Oliveira *

Posted Date: 12 July 2024

doi: 10.20944/preprints202407.0967.v1

Keywords: hydrolytic aging; natural fibre composites; rice husk; olive pit; thermo-oxidative degradation

 doi:10.20944/preprints202407.0967.v1

Article

Assessment of Long-Term Water Absorption on Thermal, Morphological and Mechanical Properties of Polypropylene-Based Composites with Agro-Waste Fillers

Tatiana Zhiltsova [1], Andreia Costa [2] and Mónica S. A. Oliveira [1,*]

[1] Mechanical Engineering Department, University of Aveiro, Aveiro, Portugal; TEMA - Centre for Mechanical Engineering and Automation, University of Aveiro, Aveiro, Portugal; LASI—Intelligent Systems Associate Laboratory,4800-058 Guimarães, Portugal; tvzhiltsova@ua.pt

[2] OLI-Sistemas Sanitários, S.A. Travessa de Milão, Esgueira, 3800-314 Aveiro, Portugal; andreiac@oli-world.com

* Correspondence: monica.oliveira@ua.pt

Abstract: Agro-waste fibres for polymer composite reinforcement have gained increased interest in industry and academia as a more sustainable alternative to synthetic fibres. However, natural fibre composites (NFC) hygroscopicity is still an issue that needs to be solved. This work investigates how prolonged exposure to water affects the properties of the polypropylene (PP)--based injection moulded composites reinforced with different contents of rice husk (rh) and olive pit (op) fibres. Both rh and op composites became more hydrophilic with increased fibre charge due to the affinity of cellulose and hemicellulose OH groups. Meanwhile, lignin contributes to the protection of the composites from thermo-oxidative degradation caused by water immersion. The PPrh composites had a higher saturation water content of 1.47% (20 wt.% rh) and 2.38 (30 wt.% rh) in comparison to PPop composites with absorption of 1.13% (20 wt.% op) and 1.59% (30 wt.% op). Tensile elastic modulus has slightly increased, at the cost of increased saturated composites' rigidity, in composites with 30% rh and op fibre content (up to 13%) while marginally decreasing (down to 8%) in PP30%op compared to unsaturated counterparts. A similar trend was observed for the flexural modulus, enhanced up to 18%. However, rh and op composites with 30% fibre content ruptured in bending, highlighting their fragility after hydrolytic ageing.

Keywords: hydrolytic aging; natural fibre composites; rice husk; olive pit; thermo-oxidative degradation

1. Introduction

A need to procure more eco-friendly solutions to guarantee the growing consumption patterns of modern society, striving at the same time to achieve carbon neutrality by 2050, requires reconsidering one's reliance on petrochemical feedstocks as a source of raw materials [1]. Simultaneously, modern society generates a huge amount of waste related to food production, which, if not properly disposed, may aggravate more the pollution problem. Reutilization of food industry waste by incorporating it into long/medium life consumer goods serves as temporary storage of carbon sequestered from the atmosphere during the growth phase [2]. Annually, Portuguese agro-industry required to dispose of more than 30,000 tons of rice husk, subproduct of paddy rice[3] and even larger quantity of olive pits, residue from olive oil extraction [4]. These agro-waste hold a huge potential for storing carbon, if incorporated into long-life products.

The replacement of synthetic polymers with their bio-based counterparts is gaining increased attention from academia and industry. However, the wholesale solution for the complete replacement of petrochemical polymer by 100% biopolymer is unlikely at present because of associated costs and market availability. For the intermediate solution in the form of natural fibre composites, a considerable body of research exist [3–5]. However, natural fillers, despite possessing some useful traits such as lower density and less abrasiveness comparable to synthetic fibres' specific

 doi:10.20944/preprints202407.0967.v1

strength and stiffness properties, are prone to thermal and mechanical degradation during processing. Another disadvantage of incorporating natural filler into the polymer matrix is their difference in polarity, as it is the case for apolar polyolefins. It is well known that hydrogen bonding sites in the natural fibres are polar, which is the main cause of their hygroscopicity and fibres' agglomeration, which may be a limiting factor for some applications [14,15]. Despite the latter limitations, the choice of polyolefins as a matrix for natural fibre composites may be attributed to their low cost, good mechanical properties, and the possibility of being processed below the degradation temperature of natural fibres by industrial processing techniques such as compression and injection moulding [16]. Moisture absorption mechanisms in natural fibre composites (NFC) are well-documented in the literature. For polyolefins, in the majority of cases, it follows the Fickian diffusion model, in which kinetic indicates a linear correlation between a fibre charge and quantity of absorbed moisture [14,16–22]. Meanwhile, moisture absorption's influence on NFC's mechanical properties may vary depending on the liquid type, temperature, test duration, and specimen preconditioning after saturation. Most of the studies claim deterioration of the mechanical properties, especially aggravated after immersion at high temperature [16,18,20,22].

Generally, the effect of moisture absorption is assessed in terms of mechanical performance. However, to the authors' knowledge, only one study [23] exists about the impact of moisture absorption on thermal stability, and no research has been found concerning the thermo-oxidative stability of hydrolytically aged NFC. Information about NFCs' thermal and thermo-oxidative stability is vital for understanding how service conditions may affect their service life expectancy.

It is worth noting that this study was carried out in the framework of the project "OLIpush—Redesign for greater circularity and a smaller environmental foot-print" which main objective is to identify an eco-friendly biopolymer capable of satisfying the requirements of functional products such as sanitary components. Hence, the present research aimed at evaluating the effect of moisture on the mechanical, thermal and morphological properties of the rice husk and olive pit polypropylene composites to verify their functional requirements for the production of sanitary components.

2. Materials and Methods

2.1. Materials

Polypropylene-based natural fibre composites with 20% and 30% by weight of rice husk and olive pits fibres were compounded by extrusion. The composites' preparation method is not reported there, given that it was described in detail in the prior research [24]. The composites' designations and compositions used along the text are listed in Table 1.

Table 1. Materials' compositions [24.]

Designation	Composition (%)			
	PP[1]	Rice Husk	Olive Pits	PPMA[2]
PPv	100	-	-	-
PP20%rh	79	20	-	1
PP30%rh	69	30	-	1
PP20%op	79	-	20	1
PP30%op	69	-	30	1

[1] 205CA-40—Polypropylene Random Copolymer by INEOS Olefins & Polymers Europe. [2] EXXELOR™ PO 1020 Maleic anhydride functionalized polypropylene.

2.2. Methods

2.2.1. Specimens' Manufacture

The dog-bone (Type I) specimens for tensile [25] and beam-type specimens (127 × 12.7 × 6.35 mm) for flexural testing [26]were fabricated by injection moulding (injection moulding machine

 doi:10.20944/preprints202407.0967.v1

Euroinj D—065, Lien Yu Machinery Co., Ltd. (Tainan City, Taiwan). A more detailed description of the specimens' preparation may be consulted elsewhere [24].

2.2.2. Water Absorption Tests

Before immersion in distilled water at room temperature (23°C±1), the tensile and flexural specimens of the composites and virgin PP were kept in an oven with ventilation for 24 h at 50 °C and afterwards cooled down to 23°C in a desiccator (HC 200 Humidity Control Cabinet by Guangdong SIRUI Optical Co., Ltd., Guangdong, China) to remove the moisture that might be absorbed from the environment. After conditioning, the initial (dry) weight was measured with a high-precision scale with a resolution of 0.01mg (an A&D GH-252 scale, A&D Company Limited, Tokyo, Japan).

During immersion, the specimens were removed and weighed at specific intervals: 24 hours, 1 week and afterwards every 2 weeks until reaching a state of effective moisture equilibrium, which is attained, according to ASTM D5229/D5229M [27], when the average moisture content of the material does not vary more than 0.02% between two consecutive reference time spans. The stainless-steel mesh barriers, shown in Figure 1, were incorporated into the beakers to prevent the specimens from floating.

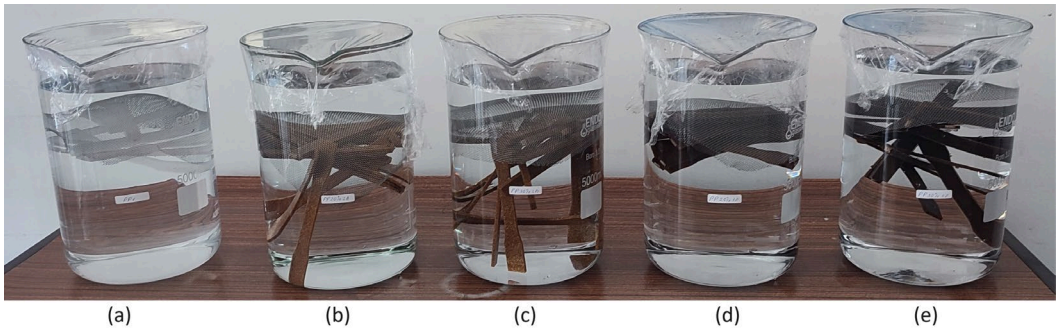

Figure 1. Experimental arrangement of the water absorption tests: (a) PPv, (b) PP20%rh, (c) PP30%rh, (d) PP20%op, (e) PP30%op.

The weighing was carried out within 2 minutes to avoid errors due to desorption. Eight tensile and flexural specimens of each material lot were tested to ensure statistical significance. After reaching the moisture equilibrium condition, the tensile and flexural specimens were removed from the immersion beakers, immediately dried, and stored in a vacuum-sealed plastic bag to avoid desorption. The mass of moisture (M) was evaluated by calculating the change in the sample mass to its original mass according to the following Equation 1 [28].

$$M = \frac{(M_t - M_0)}{M_0} 100\% \quad (1)$$

where M_t is the specimen mass at time t and M_o is the initial oven dry mass of the specimen before immersion in water.

The thickness of the tensile specimens was measured using the high-precision digital callipers from Mitutoyo (precision ± 0.01 mm), ensuring accurate results, to verify the swelling (S %) in the thickness direction after reaching the saturation limit (Equation 2). An average of eight measurements: before the moisture absorption test beginning and after moisture saturation content was carried out. The thickness swelling was calculated according to Equation 2.

$$S = \left(\frac{h_s - h_i}{h_i}\right) 100 \quad (2)$$

where h_i and h_s are the initial and saturated thicknesses.

Diffusion coefficient D (Equation 3), which represents water's ability to penetrate the polymer matrix, was analyzed postulating a Fickian diffusion mechanism after moisture equilibrium was attained [27,28].

 doi:10.20944/preprints202407.0967.v1

$$D = \pi \left(\frac{h}{4M_m}\right)^2 \left(\frac{M_2 - M_1}{\sqrt{t_2} - \sqrt{t_1}}\right)^2 \quad (3)$$

where: h is a specimen thickness (mm); M_m is a moisture saturation content (%): M_2 - M_1 – linear slope on moisture absorption curve at a time span, $\sqrt{t_2}$ - $\sqrt{t_1}$.

In Equation 3, water absorption is considered through the thickness (1D). However, in practice, moisture diffusion occurs from all six surfaces of the specimens under study, requiring a correction factor (Equation 4) introduced by Shen and Springer [28,29] for moisture ingression through the edges. This enables the determination of true one-dimensional diffusion coefficient D_x.

$$D_x = D\left(1 + \frac{h}{L} + \frac{h}{W}\right)^{-2} \quad (4)$$

Where W and L are length and width of the specimens (mm).

2.2.3. Thermal Analysis

The oxidative resistance of virgin PP and PP composites was determined according to ASTM D3895-14 [30]. Samples were films, obtained from the specimens and after the long-term water immersion The samples, with a mass of about 8 ± 1.5 mg, uniformly covered the bottom of the aluminium crucible without a lid. It was heated under a nitrogen atmosphere from ambient temperature up to 190 °C at a heating rate of 20 °C/min and maintained isothermally for 5 min. Next, the nitrogen was replaced by oxygen and maintained until reaching the exothermic peak.

Thermal stability of the composites was assessed by thermo-gravimetric analysis (TGA), performed in a Netzsch – Jupiter STA 449 F3 apparatus (NEDGEX GmbH, Selb, Germany) according to E 2550-11 [31]. The samples of 10±1mg were collected from the tensile tests' coupons before water immersion. They were heated in an alumina (Al_2O_3) crucible between 30°C and 600°C at a constant heating rate of 10°K/min under nitrogen atmosphere (50 mL min^{-1}) to measure weight change as a function of temperature. In addition, the DTG curve (rate of change of weight) was used to assist the interpretation of the thermal degradation events.

2.2.4. Morphology Assessment

Morphological analysis of the fractured surface of the tensile specimens was per-formed using a tabletop scanning electron microscope (SEM) HITACHI TM4000Plus (Hitachi High-Tech Corporation, Tokyo, Japan). The SEM images were acquired at an accelerating voltage of 15 kV.

Assessment of the composites' surface morphology was carried out under a magnification of 20 by Inspectis HD-009 DIM-U Digital Inverted Microscope (DIM) 8.3MP Ultra HD (Inspectis AB, Kista, Sweden).

 doi:10.20944/preprints202407.0967.v1

2.2.5. Tensile and Flexural Tests

Before mechanical testing, the water-saturated tensile and flexural specimens were kept in vacuum-sealed plastic bags to avoid moisture desorption. The Young's modulus and ultimate tensile strength of the samples were assessed using an X-10kN machine (Shimadzu Scientific Instruments, Columbia, MD, USA) following respectively the ISO 527-1 [30] and ISO 178 [31] standards. Eight Type I specimens were subjected to the tensile tests. The experiments were carried out at an ambient temperature (23 ± 1°C) in two steps. Initially, the specimens were pulled at a of 1 mm/min rate to calculate Young's modulus. In the second stage, a 50 mm/min tensile rate was applied and maintained until the specimens ruptured. The data from this second test were used to determine the ultimate tensile strength (σ_u) and tensile strain at break (ε_b). Flexural testing (3-point bending) was performed at a 5 mm/min speed. The beam-type test specimen with dimensions of 127 × 12.7 × 6.35 mm follows the ISO 178 [31] requirement of 20 ± 1 of the length to the thickness ratio.

3. Results and Discussion

3.1. Long-Term Water Absorption Tests

Polymer composites reinforced with natural fibres have poor resistance to moisture due to surface-abundant hydroxyl groups, present in plants fibres, possessing high polarity as well and allowing for interactions between free hydroxyl groups on fibres surface and water molecules via hydrogen bonding [32]. The difference in polarity between polymer matrix and natural fibres causes poor polymers' wetting of the latter and hence weak interface adhesion [33]. The water absorption was plotted versus the square root of time for the tensile (Figure 2) and the flexural specimens (Figure 3). At first, it increases linearly and then levels off during a long time until reaching the equilibrium following a Fickian diffusion curve. This moisture absorption behaviour of natural fibre composites has been referred in many studies [17–19]. The moisture saturation equilibrium was reached in 272 days for all rh and op composites independently of the fibre content. As expected, the hydrophobicity of PP results in negligible water absorption (Figure 2) of 0.02% [34].

It is well known that hydrogen bonding sites in the natural fibres, mostly cellulose and hemicelluloses are the main cause of their hygroscopicity and hence an increase in fibre percentage will promote water absorption [19,20]. Hence, the highest moisture saturation content (M_m) of 2.38% (**Table 2**,) recorded for PP30%rh is to be expected. In general, rice husk fibres contain more hemicellulose and have more porous structure than olive pit fibres which makes them more hydrophilic [35]. In addition, weak interlocking between the matrix and rice husk fibres elongated planar shape [24] allows for large contact area with moisture when it permeates micro cracks in polymer matrix and reaches the rh fibre. In their turn, olive pit fibres are particle-shaped which decreases their exposure-area to moisture leading to higher resistance to water uptake, being the tensile specimens PP30%op the worst-case scenario with 1.59% water absorption. An increase in thickness, which is the case for flexural specimens, decreased the water absorption in all the composites tested. The diffusion coefficient represents the ability of water molecules to move between polymer chains. The smallest diffusion coefficient was correlated with higher equilibrium saturation of PP30%rh tensile specimen. It can be attributed to continuous filling of more hygroscopic sites of the rice husk fibres, while diffusion speed through the matrix was constrained [36].

 doi:10.20944/preprints202407.0967.v1

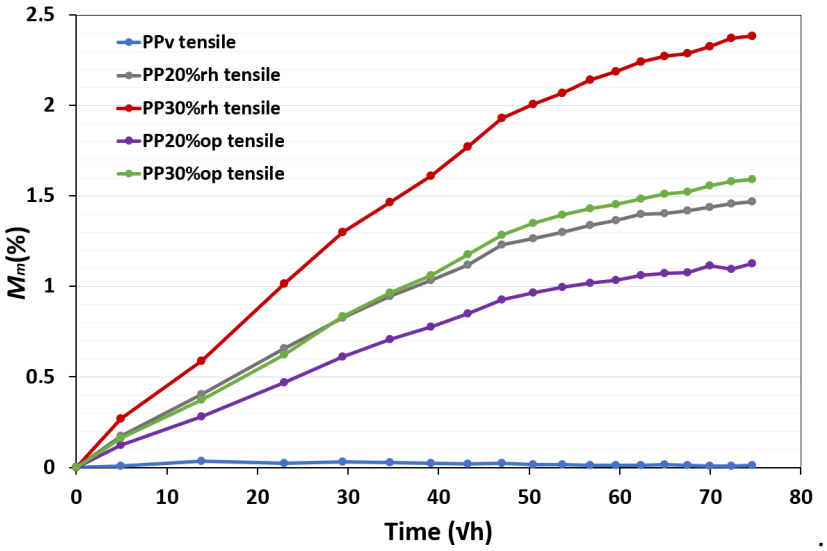

Figure 2. Water absorption behaviour (tensile specimens).

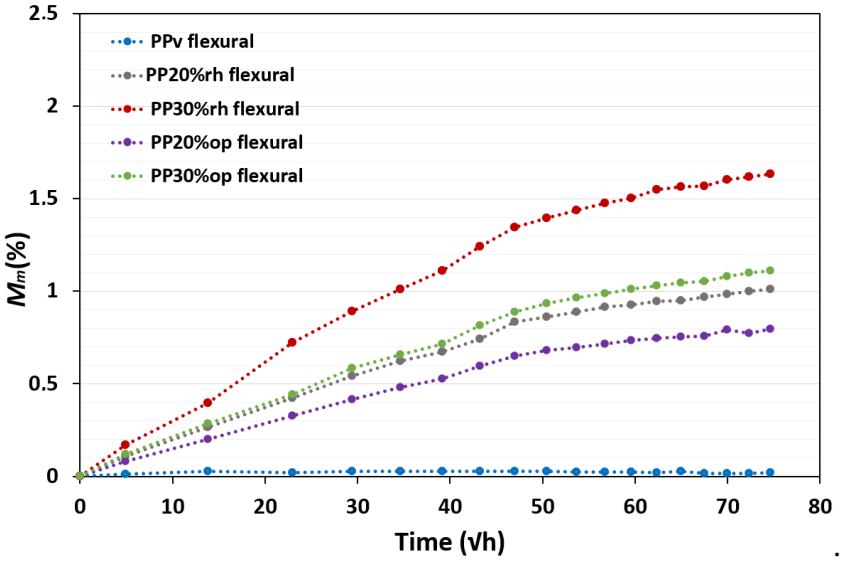

Figure 3. Water absorption behaviour (flexural specimens).

Table 2. Water absorption properties.

Property	Specimen type	PP20%rh	PP30%rh	PP20%op	PP30%op
Moisture saturation content - M_m (%)	TS[1]	1.47	2.38	1.13	1.59
	FS*	1.01	1.63	0.80	1.11
Diffusion coefficient - D_c (x 10^{-7}) (mm^2/s)	TS	1.153	1.147	1.216	1.166
	FS	2.764	3.134	2.798	2.572
Time to saturation (days)	TS	272	272	272	272
	FS	272	272	272	272

[1] TS and FS stands for, respectively, tensile and flexural specimens.

The thickness swelling of the composites was assessed only for the tensile specimens. It should be noted that the op composites' tensile specimens are thicker (Figure 4), than the rh specimens due to the higher density of the former, reported in the previous research [24]. The thickness swelling after water saturation is proportional to the equilibrium water absorption (**Table 2**), being highest

 doi:10.20944/preprints202407.0967.v1

(1.9%) for PP30%rh and lowest (0.8%) for PP20%op after immersion in distilled water for 272 days at room temperature. Higher fibre content was also positively correlated with swelling thickness for all the composites.

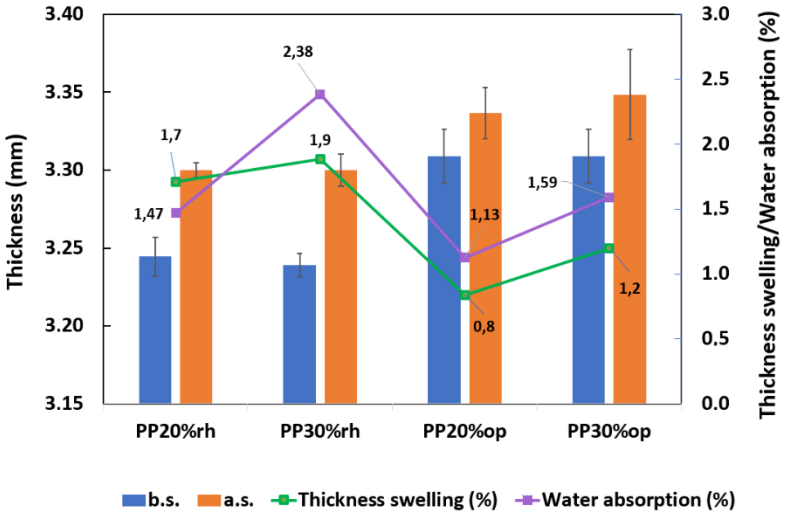

Figure 4. Thickness swelling of composites tensile specimens.

3.2. Thermal Properties

3.2.1. Oxidation Induction Time

Oxidation induction time measurements were carried out to compare the oxidative resistance at 190 °C of the composites and virgin PP before and after water immersion. The results, listed in**Table 3**, show that before water immersion, PPv and PP30%op were the most resistant to thermo-oxidative degradation, occurring at 18s and 20s, respectively. A direct correlation between the filler content increase and OIT of the op composites was established. Thus, it is reasonable to conclude that the olive pit fibres improve the OIT, delaying the oxidation mechanisms of the PP matrix, especially with a higher filler charge (PP30%op), where the OIT was superior of that of the PPv. Meanwhile, the rh composites have a thermo-oxidative resistance of 10s, invariant from the filler amount. These filler-type-related differences can be attributed to higher lignin content in olive pit fibres, which acts as a natural antioxidant [32]. Lignin is also present in rice husk fibres, but in lesser amounts [37]. The high thermal stability of lignin due to its chemical structure was reported to improve the oxidative stability of recycled PP [38] and flax fibre HDPE composites [39].

After water immersion, the oxidative resistance of PPv drops almost four-fold. This drastic reduction may be due to the partial consumption of antioxidants during the processing of specimens and hydrolytic ageing. The latter hypothesis is in line with the findings of Massey et al. [40] They have concluded that hydrolytic aging was caused by oxidation of PP surface at 9–10 nm depth. The rh and op composites' oxidative stability have also decreased after aging in water but by a lesser degree. Thermo-oxidative degradation of the composites may be promoted by leaching of soluble and insoluble fibre substance into water, as it was observed during the water immersion test (Figure 5) resulting in the specimens' surface erosion. Water leaching of soluble and insoluble substances from the fibres, is a well-known problem for natural fibre composites which weakens the fibre/matrix interface and deteriorates their mechanical properties [41,42]. Surface erosion caused water leaching may aggravate the previously discussed hydrolysis of the polypropylene matrix. It is worth mentioning that the higher fibre amount and, hence, lignin content significantly dampened the composites' thermo-oxidative degradation being directly correlated with the OIT reduction.

 doi:10.20944/preprints202407.0967.v1

Table 3. Oxidation Induction Time before and after water immersion.

Material	OIT (s)		OIT↓ (%)[1]
	before immersion	after immersion	
PPv	17.8± 2.5	4.5± 0.2	75
PP20%rh	10.2± 0.5	5.9± 0.6	42
PP30%rh	10.4± 0.8	8.0± 0.8	23
PP20%op	14.3± 0.1	8.6± 0.6	40
PP30%op	19.6± 1.8	12.2± 1.1	38

[1] OIT↓ (%) stands for oxidative induction time reduction before and after water immersion.

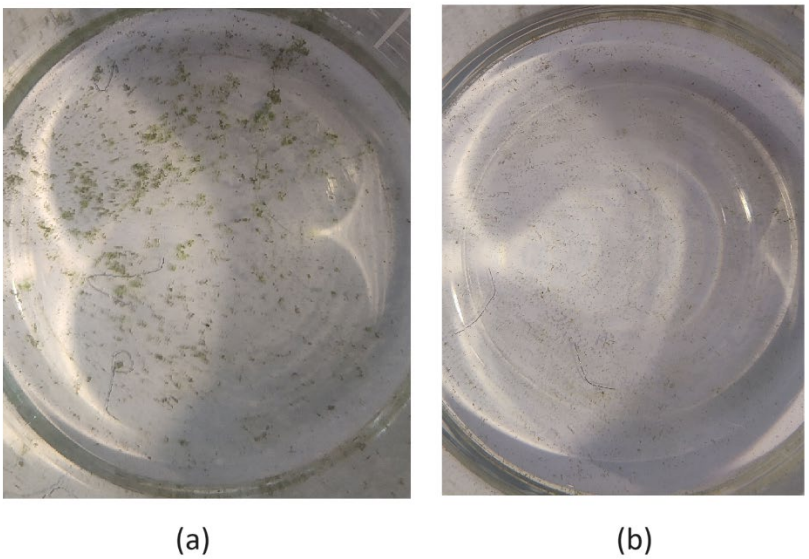

Figure 5. Residue of the insoluble fibre substance deposited at the bottom of the immersion beaker: (a) PP30%rh, (b) PP30%op.

3.2.2. Thermogravimetric Analysis (TGA) and Derivative Thermogravimetry (DTG)

Thermogravimetric analysis under an inert atmosphere was carried out to investigate the effect of the natural fibre reinforcement on the thermal stability of the composites and the assessment of their filler content. The presence of organic fillers, composed from cellulose, hemicellulose and lignin, makes these composites especially prone to thermal degradation, limiting the processing temperature range[11].

Hence, it is vital to understand their performance under high temperatures. The results are presented in Figure 6, Figure 7 and **Table 4**. Virgin PP co-polymer underwent a single thermal event. It started to degrade at 313.7°C (T_i), having only one peak (DTG max) in the derivative thermogravimetric curve (Figure 7) at 448.2°C, designated in **Table 4** as $T_{DTG\ 2nd.peak}$. The ash content changes very slightly after 500°C, volatilizing the PPv almost completely (0.8% ash content) at 600°C, corroborating the data reported by other researchers [43]. PPv's nearly complete thermal destruction may be attributed to polymer chains' molecular scission and high-temperature volatilisation[44] [45].

The weight loss occurs in several stages for the rice husk and olive pit composites. At the first barely perceptible stage, between the initial test temperature (30°C) and the onset temperature of the first stage (T_i) about 1% of the weight is lost due to water evaporation (Figure 6). No moisture evaporation was detected for PPv due to its hydrophobic nature. According to the DTG thermograms depicted in Figure 7, the thermal degradation of the rice husk and olive pit composites occurs in two stages. There are two temperature peaks in the first stage, in which the onset temperatures vary from 219°C to 234°C as a function of the filler's amount and type (**Table 4**), indicating that the composites with a lower fibre content are more thermally stable. Regarding the influence of filler type, op composites showed a marginal advantage. It should be noted that in **Table 4**, only clearly identifiable

 doi:10.20944/preprints202407.0967.v1

temperature peaks were listed. The temperature interval between 220°C and 310°C can be attributed to the decomposition of hemicellulose. The first peaks occurring in the interval between 310°C and 380°C, as highlighted in Figure 7, are due to the destruction of cellulose [11,46] .

In the second stage with the onset temperature varying for rh composites (373°C) and op composites (376°C), the maximum weight loss rates happened in a range of 455-457°C, several degrees higher than in virgin PP, indicating that beside the PP matrix decomposition, the lignin decomposition, which reported to have a more thermally stable polyaromatic structure than hemicellulose and cellulose gradually decomposing over broad temperature range, is also present at this stage [43,47] .

Once the temperature reaches 500°C, a significant stage is reached as the degradation process is generally complete. At this point, most of the polymer matrix and fibre' constituents have been already pyrolyzed and converted to gases and ash. The residual ash content, which provides indirect information about the fibre content in the composites, is a key indicator of this stage. As shown in **Table 5**, the fibre content is proportional to the ash content, independently of the fillers' type. The higher rate of the ash residue in the rh composite in comparison to the op composites is due to the rice husk's silica content, which was maintained untransformed in the ash [48] as its decomposition temperature is higher than the temperature range used during the TGA test. Moreover, in all the composites the ash residue content changes with the same rate as the amount of the filler.

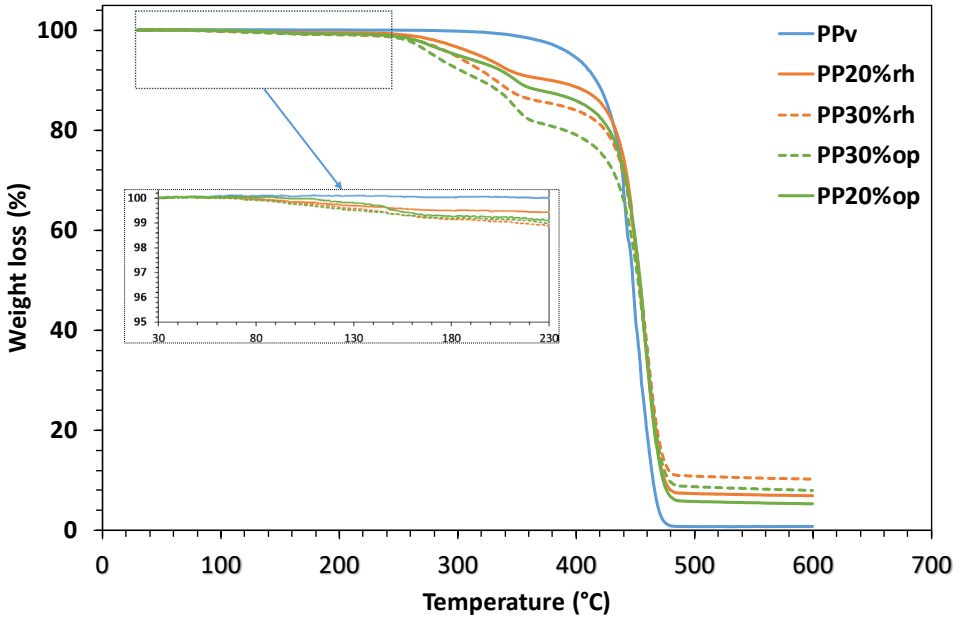

Figure 6. TGA thermograms of PPv and rice husk and olive pit biocomposites.

Preprints.org (www.preprints.org) | NOT PEER-REVIEWED | Posted: 12 July 2024 doi:10.20944/preprints202407.0967.v1

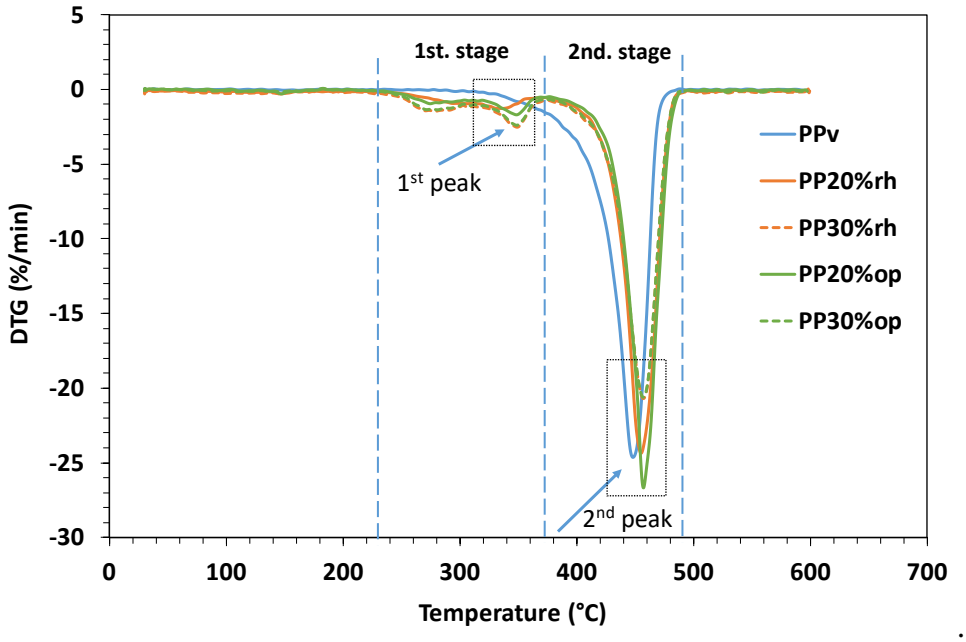

Figure 7. DTG thermograms of PPv and rh and op composites.

Table 4. Thermal decomposition data of the PPv and the composites.

Material	1st stage			2nd stage			Ash residue[5](%)
	T_s[1]- T_e [2] (°C)	$T_{DTG\ 1st.peak}$(°C)	Weight loss[3] (%)	$T_s - T_e$ (°C)	$T_{DTG\ 2nd.peak}$ (°C)	Weight loss [4] (%)	
PPv	—	—	—	313.7 – 486.3	448.2	99.2	0.8
PP20%rh	233.7 - 372.1	—	9.8	372.1 – 494.1	455.1	92.2	6.9
PP30%rh	219.2 – 373.9	348.9	14.4	373.9 – 498.0	457.1	89.1	10.2
PP20%op	234.1 – 376.5	348.5	12.4	376.5 – 496.4	457.1	94.2	5.3
PP30%op	221.5 – 376.3	348.6	19.0	376.3 – 497.7	457.0	91.1	8.0

[1] T_s- onset temperature; [2] T_e - end temperature; onset te[1]weight loss at the end of the 1st stage; [2]weight loss at the end of the 2nd stage; [3]ash residue at 600°C.

Table 5. Relation between the ash residue and the fibre content.

Material	F.C. (%)[1]	A.R. (%)[2]	A.R./F.C.	A.C.R.[3]
PP20%rh	20	6.9	0.35	1.5
PP30%rh	30	10.2	0.34	
PP20%op	20	5.3	0.27	1.5
PP30%op	30	8.0	0.27	

[1] F.C. - fibre content; [2]A.R. – ash residue; [3]A.C.R. is a rate between the ash content at different content of the same filler (e.g., $A.R._{PP30\%rh.}/A.R._{PP20\%rh}$).

3.3. Morphology Assessment

The fractured cross-sections of the composites' tensile specimens were analyzed with the SEM micrographs (Figure 8 and Figure 9), where the images under (c) and (d) labels represent the fractured cross-sections of the composite after immersion in water. As expected and reported in detail in the previous research for the composites before water immersion [24], uneven fibre distribution, clamping, and cracks caused by the fibre pulling during fracture are shown in all the images. A non-uniform fibres' dispersion in the PP matrix was caused by the extrusion and injection molding of the composites. So given that SEM imaging of the specimens after water immersion was carried out when the water absorbed during the immersion test had already been desorbed [49], as the specimens were

 doi:10.20944/preprints202407.0967.v1

kept under room temperature between the preparation (tensile tests) and SEM observation, it is reasonable to conclude that the absence of the visible alteration of the in-deep thickness specimens' morphology was due to desorption.

However, considering the erosion of the composites' surface during immersion, indirectly indicated by the composites' fibre leaching into the water as demonstrated in Figure 5, the major morphology alterations are to be expected at the specimens' surface. DIM micrographs were acquired to evaluate the composites' surface condition before and after water exposure (Figure 10). The left side images, labelled as (a), (c), (e) and (g), depicted the tensile specimens' surface before water immersion. As the PP matrix used for compounding the composites is translucent in its original form, the rice husk and olive pit fibres are visible under the specimens' surface. Moreover, the slight whitish strikes, aligned in the direction of mould filling, are identifiable with different intensities in all the images mentioned above, indicating specimens' surface abrasion by fibres during injection moulding. These surface defects were aggravated after the long-term water immersion, as shown in Figure 10 right side images (b), (d), (f), and (h), where these whitish strikes appear to gain in-depth, by water leaching of soluble and insoluble substances from the fibres as evidenced in Figure 5. The whitening of the rice husk fibres under the specimen surface Figure 10 (b), (d) due to water leaching further corroborates this hypothesis. Meanwhile the op composites are less prone to water leaching, as less insoluble fibre residue deposition was detected at the end of the immersion test (Figure 5 (b)). However, they appear to be more abrasive especially with higher filler content (Figure 10 (g) and (h)).

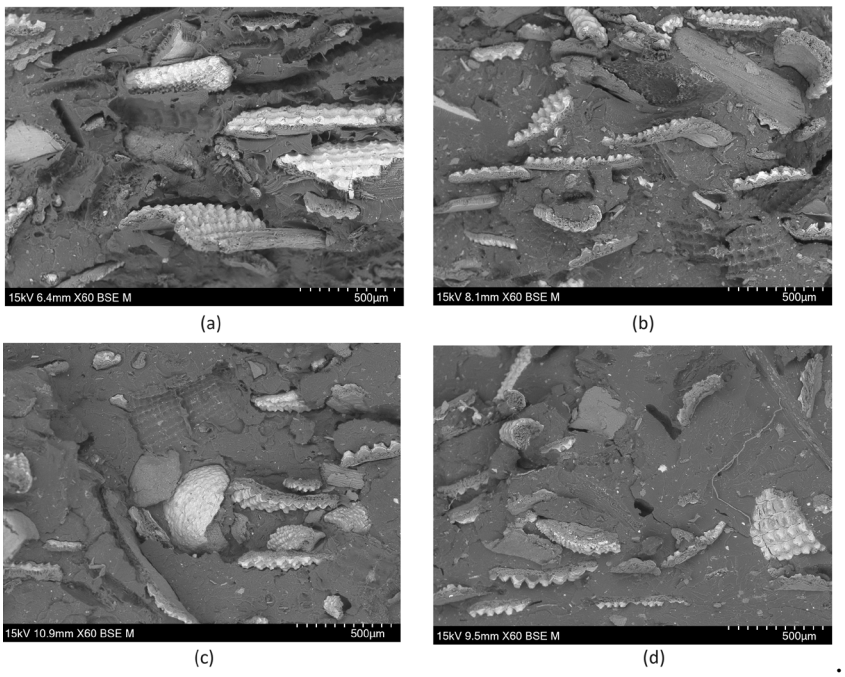

Figure 8. SEM micrographs: (a) PP20%rh_b.i., (b) PP30%rh_b.i., (c) PP20%rh_a.i., (d) PP30% rh_a.i..

 doi:10.20944/preprints202407.0967.v1

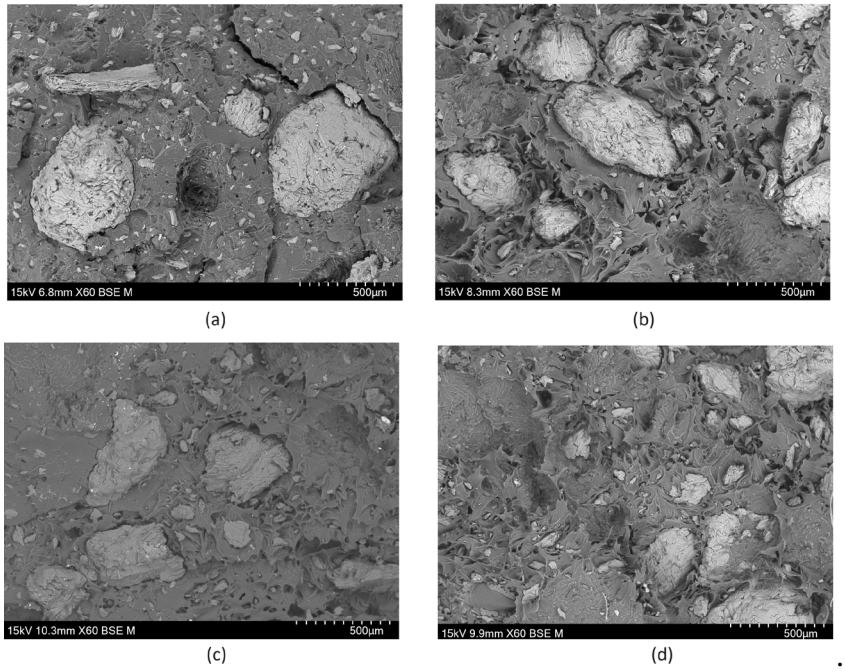

Figure 9. SEM micrographs: (a) PP20%op_b.i., (b) PP30%op_b.i., (c) PP20%op_a.i., (d) PP30% op_a.i..

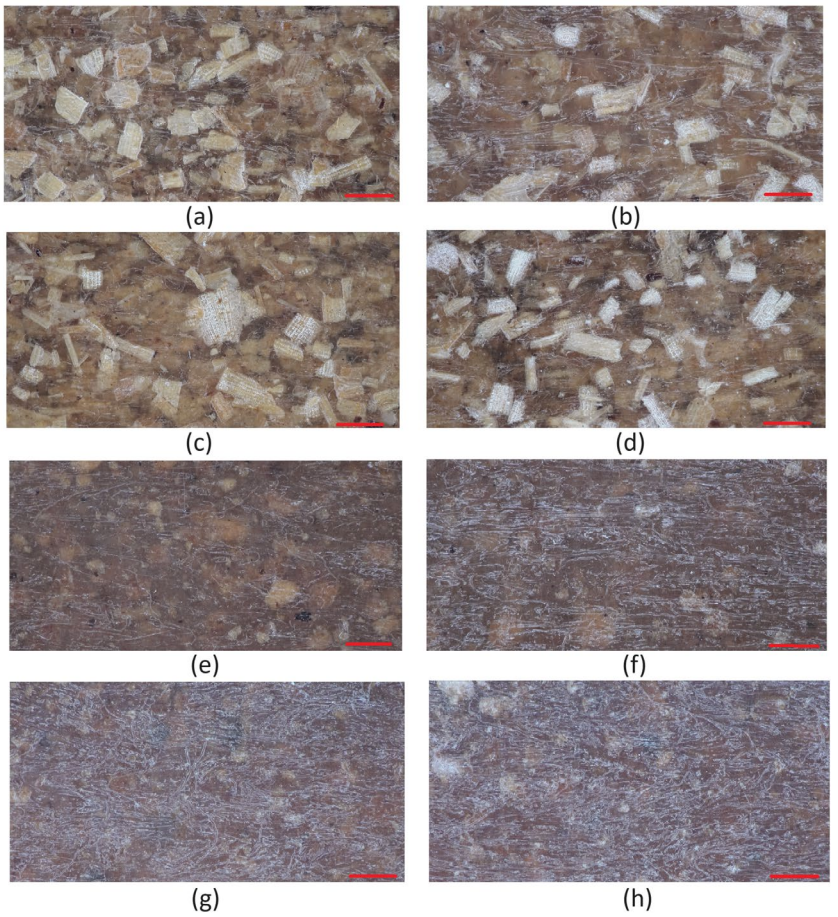

Figure 10. DIM micrographs: (a) PP20%rh_b.s., (b) PP20%rh_a.s., (c) PP30%rh_b.s., (d) PP30%rh_a.s., (e) PP20%op_b.s., (f) PP20%op_a.s., (g) PP30%op_b.s., (h) PP30%op_a.s. (red scale bar is equal to 1000 µm).

 doi:10.20944/preprints202407.0967.v1

3.2. Influence of Water Absorption on the Mechanical Properties

Before tensile and flexural testing, the water-saturated specimens were preserved in vacuum-sealed bags to prevent desorption. This procedure was adopted to emulate high humidity bathroom conditions, the intended ambient conditions for functional products such as sanitary components for which the composites under investigation are intended as more eco-friendly alternatives. As the evaluation of the dry composites' fibre type and content on their mechanical properties of composites was analyzed and reported elsewhere [24] , this assessment will be solely focused on the impact of water absorption on the mechanical properties by comparing dry and wet counterparts. As it may be seen from **Table 6** and Figure 11, the elastic modulus has decreased slightly in both rh and op 20% wet composites. However, this trend was inverted for higher fibre loading. The tensile strength was improved between 8 and 15 % with more pronounced improvement for lower fibre content. It may be attributed to the plasticizing effect of water infiltration into the microcracks at the fibre matrix interface and to fibre swelling [18,50]. However, the inverse correlation between the improved tensile strength and the fibre amount may be due to more pronounced superficial erosion of the wet specimens with 30% fibre charge. The surface damage may counteract the water and fibre swelling plasticization effect. The vindication of this possibility is a drastic reduction (39%) of the elongation at break in wet PP30%rh, where the specimen's surface show more significant wear induced by long-term water exposure Figure 10 (b). Other wet composites underwent a significant but less drastic reduction in elongation at break.

Table 6. Mechanical properties under tension.

Material	S.C.[1]	E (MPa)	ΔE (%)	σ_u (MPa)	σ_u ↑[3] (%)	ε_b (%)	ε_b ↓ (%)[4]
PP20%rh	b.i.	1377.0 ± 198.2	-0.8	19.7 ± 0.4	15.3	8.6 ± 1.2	15.5
	a.i.	1366.6± 59.5		22.7 ± 0.4		7.2 ± 0.9	
PP30%rh	b.i.	1322.6 ± 170.63	6.9	19.6 ± 0.6	8.4	8.3 ± 1.4	38.9
	a.i.	1413.73± 43.5		21.3 ± 0.2		5.1 ± 0.4	
PP20%op	b.i.	1305.8 ± 217.8	-7.8	18.6 ± 0.5	11.4	10.0 ± 1.7	14.9
	a.i.	1204.3± 34.1		20.7 ± 0.5		8.4 ± 0.9	
PP30%op	b.i.	1249.6 ± 239. 8	13.3	16.6 ± 0.3	8.1	6.8 ± 1.1	19.7
	a.i.	1416.02± 106.1		17.9 ± 0.4		5.5 ± 1.0	

[1] S.C. – specimen's condition: (b.i.) – before immersion; (a.i.) – after immersion; [2] Δ—difference; [3] ↑—increase; [4] ↓—decrease.

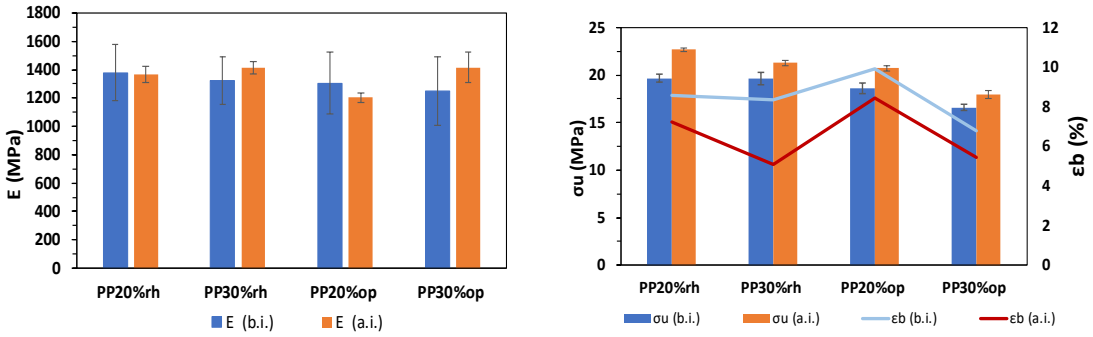

(**a**) (**b**)

Figure 11. Mechanical properties of the composites under tension: (a) elastic modulus; (b) σ_u and ε_b.

After long-term water exposure, the composites' flexural modulus and strength were improved by 3% -18% and 4%-11%, respectively, as envisaged in Figure 12 (a) and (b) and **Table 7**. It should be noted that both flexural modulus and strength follow the same trend as the tensile strength, showing more significant improvement at lower fibre charge. A more modest increase in the wet specimens' flexural modulus and strength with higher fibre charge may be explained by the same conjugation of

 doi:10.20944/preprints202407.0967.v1

water-induced filling of micro crack sand fibre swelling and more significant water-induced specimens' surface damage. It is worth mentioning that in three-point bending mode, the force is applied locally to the surface damaged by water exposure, which at 30% op and rh filler content led to the specimens' fracture at ultimate flexural strength (σ_{uf}) of 23MPa for PP30%rh and 11MPa for PP30%rh.

Table 7. Mechanical properties under bending.

Material	S.C.[1]	E_f (MPa)	↑E_f(%)	σ_f (MPa)	σ_f ↑[3] (%)	σ_{uf} (MPa)
PP20%rh	b.i.	1263.4 ± 77.1	17.6	30.3 ± 0.8	11.3	—
	a.i.	1485.5 ± 16.0		33.7 ± 0.2		—
PP30%rh	b.i.	1572.4 ± 67.0	3.3	31.4 ± 0.9	5.1	—
	a.i.	1624.1± 17.6		33.0 ± 0.3		22.7 ± 3.1
PP20%op	b.i.	1170.5 ± 47. 3	17.2	28.6 ± 0.8	7.3	—
	a.i.	1371.7± 25.0		30.7 ± 0.3		—
PP30%op	b.i.	1356.5 ± 95.5	13.9	29.0 ± 1.4	3.9	—
	a.i.	1544.8 ± 22.9		30.1 ± 0.3		11.3 ± 1.5

[1] S.C. – specimen's condition: (b.i.) – before immersion; (a.i.) – after immersion; [2] Δ—difference; [3] ↑—increase; [4] ↓—decrease.

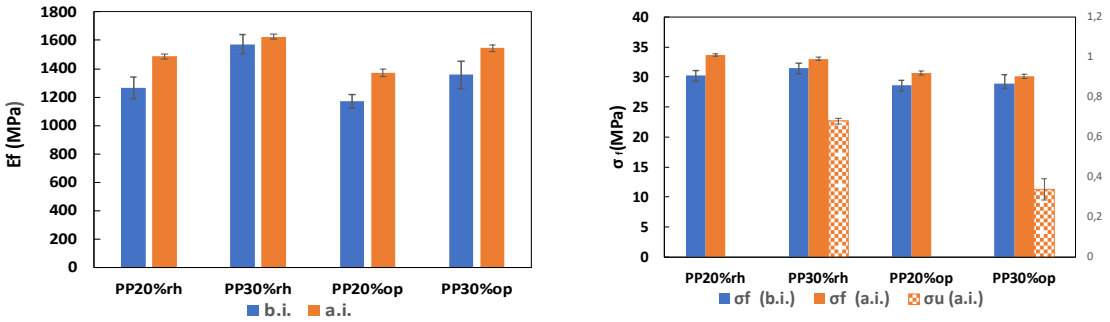

(**a**) (**b**)

Figure 12. Mechanical properties of the composites under bending: (a) flexural elastic modulus; (b) flexural strength (σ)–and ultimate stress at break (σ_{uf}).

5. Conclusions

The impact of water absorption at room temperature on the mechanical, thermal and morphological properties of the injection moulded polypropylene composites with endogenous rice husk and olive pit fibre has been studied. The water absorption followed Fickian behaviour for all the composites and took nine months to reach an equilibrium saturation state. Rice husk composites were more prone to water absorption and thickness swelling, which was less than 2% for the maximum water absorption. Long-term water exposure significantly decreased the thermo-oxidative stability of virgin PP. Meanwhile, lignin in rice husk and olive pit fibres dampened the composites' thermo-oxidative degradation caused by water immersion. Lower filler content is correlated with the rh and op composites' higher thermal stability, widening their temperature processing range. Exposure to water results in a slight increase of the tensile and flexural properties, making the composites, however, more brittle, especially critical at a higher filler content. The latter was caused by the degradation of the fibre–matrix interface at the specimens' surface, observed by microscopy. Attending the project's objectives, where this study belongs, the most promising candidate for substituting synthetic polymer in technical, sanitary components is a 20% olive pit fibre composite. It aligns low moisture absorption, dimensional stability, and resistance to thermo-oxidative degradation. In addition, hydrolytic ageing causes lesser deterioration of the mechanical properties of PP20%op in comparison to other NFC composites under investigation.

Author Contributions Conceptualization. T.Z. and M.S.A.O.; data curation. T.Z.; formal analysis. T.Z. and M.S.A.O.; funding acquisition. A.C. and M.S.A.O.; investigation. T.Z. and M.S.A.O.; methodology. T.Z. and M.S.A.O.; project administration. T.Z. and M.S.A.O.; resources. T.Z.. A.C. and M.S.A.O.; supervision. M.S.A.O.; validation. T.Z. and M.S.A.O.; writing—original draft. T.Z.; writing—review and editing. T.Z. and M.S.A.O. All authors have read and agreed to the published version of the manuscript.

Funding: Please add: "The present study was developed in the scope of the Project "Agenda ILLIANCE" [C644919832-00000035|Project nº 22]. financed by PRR—Plano de Recuperação e Resiliência under the Next Generation EU from the European Union. The present study was supported by TEMA: UIDB/00481/2020 (DOI 10.54499/UIDB/00481/2020) and UIDP/00481/2020 (DOI 10.54499/UIDP/00481/2020).

Data Availability Statement: All data generated or analyzed during this study are included in this article.

Acknowledgments: T. Zhiltsova is grateful to the Portuguese national funds (OE). through FCT. I.P.. in the scope of the framework contract foreseen in the numbers 4. 5. and 6 of Article 23. of the Decree-Law 57/2016. of August 29. changed by Law 57/2017. of July 19.

Conflicts of Interest Author Andreia Costa was employed by the company OLI-Sistemas Sanitários. S.A. The remaining authors declare that the research was conducted in the absence of any commercial or financial relationships that could be construed as a potential conflict of interest.

References

1. E. Commission and D.-G. for C. Action, *Going climate-neutral by 2050 – A strategic long-term vision for a prosperous, modern, competitive and climate-neutral EU economy*. Publications Office, 2019. doi: doi/10.2834/02074.
2. Z. Shamsollahi and A. Partovinia, "Recent advances on pollutants removal by rice husk as a bio-based adsorbent: A critical review," *Journal of Environmental Management*, vol. 246. Academic Press, pp. 314–323, Sep. 15, 2019. doi: 10.1016/j.jenvman.2019.05.145.
3. Made in EU Rice, "Sustainable EU rice." [Online]. Available: https://www.sustainableeurice.eu/sustainable-rice/
4. F. M. dos S. Foundation., "PORDATA, the Database of Contemporary Portugal." [Online]. Available: https://www.pordata.pt/en/portugal/olive+production+–+mainland+portugal-3362
5. S. Valvez, A. Maceiras, P. Santos, and P. N. B. Reis, "Olive Stones as Filler for Polymer-Based Composites: A Review.," *Materials (Basel)*, vol. 14, no. 4, Feb. 2021, doi: 10.3390/ma14040845.
6. P. Sahu and M. K. Gupta, "Water absorption behavior of cellulosic fibres polymer composites: A review on its effects and remedies," *Journal of Industrial Textiles*, vol. 51, no. 5_suppl, pp. 7480S-7512S, Nov. 2020, doi: 10.1177/1528083720974424.
7. T. P. Sathishkumar, P. Navaneethakrishnan, S. Shankar, R. Rajasekar, and N. Rajini, "Characterization of natural fiber and composites – A review," *Journal of Reinforced Plastics and Composites*, vol. 32, no. 19, pp. 1457–1476, 2013, doi: 10.1177/0731684413495322.
8. Z. N. Azwa, B. F. Yousif, A. C. Manalo, and W. Karunasena, "A review on the degradability of polymeric composites based on natural fibres," *Mater Des*, vol. 47, pp. 424–442, 2013.
9. J. S. S. Neto, H. F. M. de Queiroz, R. A. A. Aguiar, and M. D. Banea, "A Review on the Thermal Characterisation of Natural and Hybrid Fiber Composites," *Polymers*, vol. 13, no. 24. 2021. doi: 10.3390/polym13244425.
10. I. Elfaleh *et al.*, "A comprehensive review of natural fibers and their composites: An eco-friendly alternative to conventional materials," *Results in Engineering*, vol. 19, p. 101271, 2023, doi: https://doi.org/10.1016/j.rineng.2023.101271.
11. S. N. Monteiro, V. Calado, R. J. S. Rodriguez, and F. M. Margem, "Thermogravimetric behavior of natural fibers reinforced polymer composites—An overview," *Materials Science and Engineering: A*, vol. 557, pp. 17–28, 2012, doi: https://doi.org/10.1016/j.msea.2012.05.109.
12. M. Bahrami, J. Abenojar, and M. Á. Martínez, "Recent progress in hybrid biocomposites: Mechanical properties, water absorption, and flame retardancy," *Materials*, vol. 13, no. 22. MDPI AG, pp. 1–46, Nov. 02, 2020. doi: 10.3390/ma13225145.
13. H. Ku, H. Wang, N. Pattarachaiyakoop, and M. Trada, "A review on the tensile properties of natural fiber reinforced polymer composites," *Compos B Eng*, vol. 42, no. 4, pp. 856–873, 2011, doi: https://doi.org/10.1016/j.compositesb.2011.01.010.
14. A. Espert, F. Vilaplana, and S. Karlsson, "Comparison of water absorption in natural cellulosic fibres from wood and one-year crops in polypropylene composites and its influence on their mechanical properties," *Compos Part A Appl Sci Manuf*, vol. 35, no. 11, pp. 1267–1276, Nov. 2004, doi: 10.1016/j.compositesa.2004.04.004.

15. M. Tajvidi and A. Takemura, "Thermal Degradation of Natural Fiber-reinforced Polypropylene Composites," *Journal of Thermoplastic Composite Materials*, vol. 23, no. 3, pp. 281–298, Sep. 2009, doi: 10.1177/0892705709347063.
16. H. Fang, Y. Zhang, J. Deng, and D. Rodrigue, "Effect of fiber treatment on the water absorption and mechanical properties of hemp fiber/polyethylene composites," *J Appl Polym Sci*, vol. 127, no. 2, pp. 942–949, 2013.
17. A. Fotouh, J. Wolodko, and M. G. Lipsett, "Isotherm moisture absorption kinetics in natural-fiber-reinforced polymer under immersion conditions," *J Compos Mater*, vol. 49, no. 11, pp. 1301–1314, 2015, doi: 10.1177/0021998314533366.
18. E. Muñoz and J. Garcia-Manrique, "Water Absorption Behaviour and Its Effect on the Mechanical Properties of Flax Fibre Reinforced Bioepoxy Composites," *Int J Polym Sci*, vol. 2015, pp. 1–10, Oct. 2015, doi: 10.1155/2015/390275.
19. B. Kord, "Assessment of long-term water absorption in natural fiber reinforced thermoplastic composites influenced by filler rate and compatibilizer treatment," *Journal of Thermoplastic Composite Materials*, vol. 26, no. 3, pp. 296–306, 2013, doi: 10.1177/0892705711423289.
20. N. I. Ismail and Z. A. M. Ishak, "Effect of fiber loading on mechanical and water absorption capacity of Polylactic acid/Polyhydroxybutyrate-co-hydroxyhexanoate/Kenaf composite," *IOP Conf Ser Mater Sci Eng*, vol. 368, no. 1, p. 12014, 2018, doi: 10.1088/1757-899X/368/1/012014.
21. I. Naghmouchi, P. Mutjé, and S. Boufi, "Polyvinyl chloride composites filled with olive stone flour: Mechanical, thermal, and water absorption properties," *J Appl Polym Sci*, vol. 131, no. 22, 2014.
22. Z. A. Mohd. Ishak, B. N. Yow, B. L. Ng, H. P. S. A. Khalil, and H. D. Rozman, "Hygrothermal aging and tensile behavior of injection-molded rice husk-filled polypropylene composites," *J Appl Polym Sci*, vol. 81, no. 3, pp. 742–753, Jul. 2001, doi: https://doi.org/10.1002/app.1491.
23. G. B. de Seixas, H. F. M. de Queiroz, J. S. S. Neto, and M. D. Banea, "Effect of water on the mechanical and thermal properties of natural fibre reinforced hybrid composites," *J Compos Mater*, vol. 57, no. 11, pp. 1941–1958, Mar. 2023, doi: 10.1177/00219983231166570.
24. T. Zhiltsova, J. Campos, A. Costa, and M. S. A. Oliveira, "Sustainable Polypropylene-Based Composites with Agro-Waste Fillers: Thermal, Morphological, Mechanical Properties and Dimensional Stability," *Materials*, vol. 17, no. 3, p. 696, 2024.
25. International Organization for Standardization, "ISO 527-1: Plastics — Determination of tensile properties — Part 1: General principles," 2012.
26. International Organization for Standardization, "ISO 178 2001: Plastics Determination of flexural properties," 2001.
27. ASTM International, "D5229/D5229M − 14: Standard Test Method for Moisture Absorption Properties and Equilibrium Conditioning of Polymer Matrix Composite Materials," 2014.
28. G. S. Springer, "Environmental Effects," in *Engineering Mechanics of Fibre Reinforced Polymers and Composite Structures*, J. Hult and F. G. Rammerstorfer, Eds., Vienna: Springer Vienna, 1994, pp. 287–314. doi: 10.1007/978-3-7091-2702-5_11.
29. C.-H. Shen and G. S. Springer, "Moisture absorption and desorption of composite materials," *J Compos Mater*, vol. 10, no. 1, pp. 2–20, 1976.
30. ASTM International, "D3895 − 14 Standard Test Method for Oxidative-Induction Time of Polyolefins by Differential Scanning Calorimetry."
31. ASTM International, "Standard Test Method for Thermal Stability by Thermogravimetry E2550-11." doi: 10.1520/E2550-11.
32. S. F. Abdellah Ali, I. O. Althobaiti, E. El-Rafey, and E. S. Gad, "Wooden Polymer Composites of Poly(vinyl chloride), Olive Pits Flour, and Precipitated Bio-Calcium Carbonate," *ACS Omega*, vol. 6, no. 37, pp. 23924–23933, Sep. 2021, doi: 10.1021/acsomega.1c02932.
33. S. Fu, P. Song, and X. Liu, "19 - Thermal and flame retardancy properties of thermoplastics/natural fiber biocomposites," in *Advanced High Strength Natural Fibre Composites in Construction*, M. Fan and F. Fu, Eds., Woodhead Publishing, 2017, pp. 479–508. doi: https://doi.org/10.1016/B978-0-08-100411-1.00019-4.
34. A. A. Klyosov, *Wood-Plastic Composites*. Wiley, 2007. [Online]. Available: https://books.google.pt/books?id=KmuK4w_D7UUC
35. K. S. Chun, S. Husseinsyah, and N. F. Syazwani, "Properties of kapok husk-filled linear low-density polyethylene ecocomposites: effect of polyethylene-grafted acrylic acid," *Journal of Thermoplastic composite materials*, vol. 29, no. 12, pp. 1641–1655, 2016.
36. P. Siedlaczek, G. Sinn, P. Peter, R. Wan-Wendner, and H. C. Lichtenegger, "Characterization of moisture uptake and diffusion mechanisms in particle-filled composites," *Polymer (Guildf)*, vol. 249, May 2022, doi: 10.1016/j.polymer.2022.124799.
37. and L. T. V. S.D. Genieva, S.Ch. Turmanova, "Utilization of Rice Husks and the Products of Its Thermal Degradation as Fillers in Polymer Composites .," in *Cellulose Fibers: Bio- and Nano-Polymer Composites: Green*

Chemistry and Technology, Springer Berlin Heidelberg, 2011, pp. 345–377. [Online]. Available: https://books.google.pt/books?id=HZa-Ljm7iwgC

38. A. Gregorová, Z. Cibulková, B. Košíková, and P. Šimon, "Stabilization effect of lignin in polypropylene and recycled polypropylene," *Polym Degrad Stab*, vol. 89, no. 3, pp. 553–558, Sep. 2005, doi: 10.1016/j.polymdegradstab.2005.02.007.
39. L. Van Schoors, M. Gueguen Minerbe, S. Moscardelli, H. Rabii, and P. Davies, "Antioxidant properties of flax fibers in polyethylene matrix composites," *Ind Crops Prod*, vol. 126, pp. 333–339, Dec. 2018, doi: 10.1016/j.indcrop.2018.09.047.
40. S. Massey, A. Adnot, and D. Roy, "Hydrolytic aging of polypropylene studied by X-ray photoelectron spectroscopy," *J Appl Polym Sci*, vol. 92, no. 6, pp. 3830–3838, Jun. 2004, doi: 10.1002/app.20399.
41. M. M. Lu and A. W. van Vuure, "Effects of water immersion, natural ageing in sunlight and natural ageing under the shade on non-dry flax fibre reinforced composites," *Ind Crops Prod*, vol. 216, Sep. 2024, doi: 10.1016/j.indcrop.2024.118655.
42. A. Moudood, A. Rahman, A. Öchsner, M. Islam, and G. Francucci, "Flax fiber and its composites: An overview of water and moisture absorption impact on their performance," *Journal of Reinforced Plastics and Composites*, vol. 38, no. 7, pp. 323–339, 2019, doi: 10.1177/0731684418818893.
43. M. A. Hidalgo-Salazar and E. Salinas, "Mechanical, thermal, viscoelastic performance and product application of PP-rice husk Colombian biocomposites," *Compos B Eng*, vol. 176, p. 107135, 2019, [Online]. Available: https://www.sciencedirect.com/science/article/pii/S1359836818336655
44. H. S. Kim, S. Kim, H. J. Kim, and H. S. Yang, "Thermal properties of bio-flour-filled polyolefin composites with different compatibilizing agent type and content," *Thermochim Acta*, vol. 451, no. 1–2, pp. 181–188, Dec. 2006, doi: 10.1016/j.tca.2006.09.013.
45. S. M. L. Rosa, S. M. B. Nachtigall, and C. A. Ferreira, "Thermal and dynamic-mechanical characterization of rice-husk filled polypropylene composites," *Macromol Res*, vol. 17, pp. 8–13, 2009.
46. Y. H. Khraisha, "Thermal Decomposition of Olive-Solid Waste by TGA: Characterization and Devolatilization Kinetics under Nitrogen and Oxygen Atmospheres," *Journal of Power and Energy Engineering*, vol. 12, no. 03, pp. 31–47, 2024, doi: 10.4236/jpee.2024.123003.
47. B. JANKOVIĆ, M. B. RADOJEVIĆ, M. M. BALAĆ, D. D. STOJILJKOVIĆ, and N. G. MANIĆ, "THERMOGRAVIMETRIC STUDY ON THE PYROLYSIS KINETIC MECHANISM OF WASTE BIOMASS FROM FRUIT PROCESSING INDUSTRY," *Thermal Science*, vol. 24, no. 6 PART B, pp. 4221–4239, 2020, doi: 10.2298/TSCI200213191J.
48. A. A. Raheem and M. A. Kareem, "Chemical composition and physical characteristics of rice husk ash blended cement," *International Journal of Engineering Research in Africa*, vol. 32, pp. 25–35, 2017, doi: 10.4028/www.scientific.net/JERA.32.25.
49. B. K. Kandola, S. I. Mistik, W. Pornwannachai, and A. R. Horrocks, "Effects of Water and Chemical Solutions Ageing on the Physical, Mechanical, Thermal and Flammability Properties of Natural Fibre-Reinforced Thermoplastic Composites1. Kandola, B.K.; Mistik, S.I.; Pornwannachai, W.; Horrocks, A.R. Effects of Water and Chem," *Molecules*, vol. 26, no. 15, 2021, doi: 10.3390/molecules26154581.
50. H. N. Dhakal, Z. Y. Zhang, and M. O. W. Richardson, "Effect of water absorption on the mechanical properties of hemp fibre reinforced unsaturated polyester composites," *Compos Sci Technol*, vol. 67, no. 7–8, pp. 1674–1683, Jun. 2007, doi: 10.1016/j.compscitech.2006.06.019.